INTERNATIONAL JOURNAL OF HYDROGEN ENERGY XXX (2016) 1–12

Available online at www.sciencedirect.com

ScienceDirect

journal homepage: www.elsevier.com/locate/he

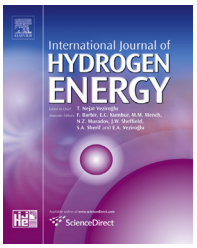

Flexible heat exchanger network design of an ethanol processor for hydrogen production. A model-based multi-objective optimization approach

Javier A. Francesconi [a,*], *Diego G. Oliva* [b], *Pio A. Aguirre* [b,c]

[a] *Instituto de Industria, Universidad Nacional de General Sarmiento (UNGS), CONICET, J. M. Gutiérrez 1150, B1613GSX Los Polvorines, Prov. de Buenos Aires, Argentina*

[b] *INGAR Instituto de Desarrollo y Diseño (CONICET-UTN), Avellaneda 3657, S3002GJC Santa Fe, Argentina*

[c] *UNL, Dpto. de Matemática, FIQ, Santiago del Estero 2829, 3000 Santa Fe, Argentina*

ARTICLE INFO

Article history:
Received 4 August 2016
Received in revised form
27 October 2016
Accepted 28 October 2016
Available online xxx

Keywords:
Ethanol processor
Energy efficiency
Flexible heat exchanger network
Hydrogen

ABSTRACT

This work addresses the optimal design of a flexible heat exchanger network using model-based optimization, applied to hydrogen production by means of an ethanol steam reforming process. High efficiencies are obtained at different hydrogen production levels ranging from 25 to 100% of a nominal output. System structure, heat exchanger sizing, and operation conditions are simultaneously settled, ensuring both operational feasibility and optimality. The system involves a reforming reactor, vaporization and reheating equipment, combustors, and a heat exchanger network system. A multi-period nonlinear optimization problem (NLP) was formulated to account for the production level distribution. Equipment sizing constraints and structural constraints link the different scenarios. The trade-off between area and efficiency is analyzed using a multi-objective epsilon-constraint approach. Models were developed in the GAMS environment. The resulting solutions, for the maximum area case, maintain alcohol combustion at low levels showing efficiencies around 63% in each operational level. Pareto Optimal diagram shows that a 1% reduction of efficiency allows a 50% decrease in total required heat exchanger area by 50%.

Introduction

In recent years, fuel cell systems fueled by hydrogen have emerged as a source of high-efficiency electric power generation. There have been several studies concerning both fuel cells and fuel processors for hydrogen generation. A fuel processor is the system that transforms feedstock fuels, such as hydrocarbons or biomass-derived fuels, into a hydrogen-rich gas. The fuel cell electrochemically converts hydrogen into electric power. Among several alternatives for hydrogen generation, ethanol reforming represents a clean and renewable source [1–4]. Bioethanol is ethanol traditionally produced by fermentation of biomass sources. Ethanol is considered the primary renewable liquid fuel [5] biotechnologically obtained from agricultural products such as sugar cane, sugar beet,

* *Corresponding author.*
E-mail addresses: jfrancesconi@ungs.edu.ar (J.A. Francesconi), doliva@santafe-conicet.gov.ar (D.G. Oliva), paguir@santafe-conicet.gov.ar (P.A. Aguirre).

http://dx.doi.org/10.1016/j.ijhydene.2016.10.156
0360-3199/

sweet sorghum, and corn starch [6]. However, these raw materials belong to the human food chain and their use in fuel ethanol production is a controversial issue. Currently, non-food-based feedstocks derived from cellulosic sources, such as wood chips and agricultural residues, present high potential for bioethanol industrial production [7,8].

Fuel cell systems for both stationary and mobile applications are highly energetic integrated systems consisting of a fuel processor, the fuel cell itself, and combustion subsystems [9,10]. Thermodynamic analysis of fuel cells systems integrated with a steam ethanol reforming processor has been performed in several works [9,11–13]. Perna [11] presents a thermodynamic analysis of the ethanol steam reforming process coupled with a proton membrane fuel cell. Applying the process energy integration approach, Francesconi et al. [9] reported that it is possible to achieve a nearly 38% energetic efficiency for an ethanol processor coupled with a proton exchange membrane fuel cell (PEMFC). A process simulation was conducted for this study, parametrically varying a set of operative variables without a defined network of heat exchangers. Subsequently, Oliva et al. [14] applied mathematical programming techniques to synthesize heat exchanger network for the fuel cell ethanol processor. In order to improve energetic efficiency new technologies based on membrane separation processes were considered [12,13]. Salemme et al. [13] analyzed the energy efficiency of an ethanol processor via simulation, indicating that the introduction of a separation membrane unit could increase global system efficiency by 5% with respect to the conventional case. These studies show the necessity for comprehensive energy integration in order to achieve a fuel processor design that is substantially more efficient than conventional technologies such as internal combustion engine.

The motivation behind this paper is the design of a flexible ethanol processor for a pilot plant scale. The function of a pilot plant system is to evaluate aspects of operability and controllability and catalysts performance; therefore one of the main targets is to achieve a flexible design that ensures operability over several hydrogen production levels. It is further desirable that efficiency maintain adequate levels over a wide range of operative conditions throughout the ethanol processor operation. In addition, these features are also applicable to fuel cell system for mobile applications where hydrogen demand is variable.

The use of process system engineering tools such as model-based optimization [15], heat exchanger networks [14], and reactor-separation networks [16], among others, has received increasing attention in fuel cell systems design [17]. Process modeling and mathematical programming are well known approaches to synthesize the process flowsheet, selecting the component parts and how to interconnect them [16]. Non-linear problem (NLP) formulation has been used for process synthesis when considering flexibility [18]. Particularly, in the fuel cell field Yunt et al. [19] propose a mathematical programming based design method to design a portable fuel cell system considering variability in the power demand levels. The method transcribes optimal operation of the system into a two-stage stochastic program that is finally reformulate as a single stage deterministic optimization problem. The development of a NLP model after applying an adequate optimization algorithm allows determining the operative variables and process configuration that maximize or minimize a given objective function.

In the process under study, heat exchangers represent the main equipment (Fig. 1). Synthesis of heat exchanger networks is one of the most widely studied problems in the area of process system engineering, given the importance of energy recovery as regards energy costs of an industrial process. The first systematic approach considering energy recovery objectives was the “pinch” concept introduced in the 1970s [20]. Later, mathematical programming techniques, stochastic optimization methods, and hybrid methods have been developed and applied to optimal design. A comprehensive review on the subject, with comments regarding flexibility and operability about heat exchanger networks, can be found in the work by Furman and Sahinidis [21].

A heat exchanger network (HEN) allows the use of energy provided by hot/cold streams in order to condition cold/hot streams of the process. Therefore, the required utilities are effectively reduced, diminishing costs and increasing energy efficiency. The design of the HEN usually starts by considering fixed operating parameters based on the process specifications under nominal conditions. In practice, the HEN must remain operational under changing conditions without losing performance specifications such as temperature and/or composition of products, while maintaining adequate levels of energy integration. When an autonomous operation of the system is desired, cold and heat utilities are not present in the HEN design. In the process under study, the heat source should be the combustion of ethanol. In other words, the energy contents of ethanol represent the only energy source of the system.

Floudas and Grossmann [22] introduced a systematic procedure for the synthesis of flexible networks of heat exchangers operating over several scenarios (periods). It is assumed that, in general, different values for flow rates and temperatures over N periods of operation are specified. The aim is to synthesize a feasible network over the N periods to achieve a minimum cost. A systematic approach in the design of heat exchanger networks under multiple operating periods is presented by Verheyen and Zhang [23]. Their methodology is based on a superstructure represented by an integer nonlinear mixed model (MINLP), which minimizes the total annualized cost including heat exchanger area and service costs. The model uses the superstructure proposed by Yee and Grossmann [24], which was formulated for multiple periods by Aaltola [25].

A bibliography revision about HEN flexibility showed that only changes in the heat capacity flow rate (mCp) or operating temperature intervals were considered across operative periods. According to our knowledge, case studies handling phase change in flexible HEN's were not analyzed in the literature. On the other hand, the use of a bypass in the heat exchanger as proposed by Aaltola [25] is not always feasible in practice. High temperatures, such as those existing in reforming operation, could technically forbid the use of valves for bypass operation.

When the operating conditions and sizing parameters are simultaneously determined, for a given heat exchanger unit, vaporization could take place in one scenario and not in any other operating period, so it is not previously known in which

Please cite this article in press as: Francesconi JA, et al., Flexible heat exchanger network design of an ethanol processor for hydrogen production. A model-based multi-objective optimization approach, International Journal of Hydrogen Energy (2016), http://dx.doi.org/10.1016/j.ijhydene.2016.10.156

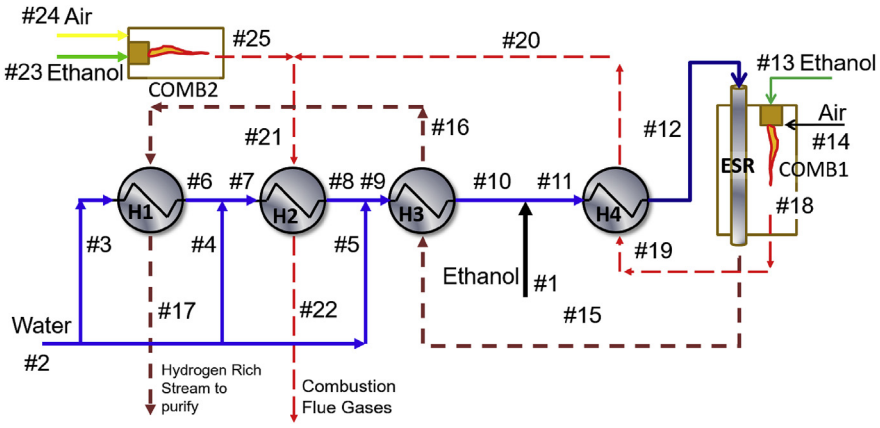

Fig. 1 – Simplified diagram of the ethanol processor. Streams and equipment.

one or more scenarios phase change might occur. Enthalpy stream determination required, a priori, known which phase is under consideration. In a mathematical programming approach, this situation can be overcome using binary variables [26,27], which incorporates combinatorial complexity to an already nonlinear and nonconvex problem. Therefore, in this work an NLP formulation is preferred and a new mathematical formulation for enthalpy calculation based on a sigmoidal approximation is presented.

This paper presents a mathematical programming approach based on a Non-Linear Problem (NLP) formulation to determine the heat exchangers area for an ethanol processor, ensuring feasible operation over different scenarios. The proposed methodology is based on applying a model-based optimization over multiple periods (scenarios) with a given structure of the heat exchangers network. A non-linear model is developed; and the obtained solution defines the heat exchanger area and operative flows and temperatures, allowing operability and acceptable levels of efficiency in each scenario.

This paper is organized as follows. A brief process description is outlined in "Process description" Section. "Optimization of problem formulation" Section presents the optimization problem formulation. In "mathematical model" Section, the mathematical model regarding the ethanol processor is described. "resolution methodology" Section presents the proposed resolution methodology and numerical aspects. The obtained results are discussed in "Results" Section. Finally, conclusions are drawn in "Conclusions" Section.

Process description

The fuel processor system is shown schematically in Fig. 1. In this work, the ethanol processor consists of a reactor for ethanol steam reforming (ESR) and four heat exchangers (H1, H2, H3, H4) with associated combustion subsystems. Raw material (water and ethanol) enters in liquid state and requires energy in order to be vaporized and reheated until reaching the reforming reaction temperature (973 K). By means of a system of bypass valves, water has the possibility of entering the system at three alternative points. The alcohol to be reformed is incorporated by being mixed with water steam before reaching heat exchanger H4. Given the autonomous feature of the system, the energy required for vaporization and reforming reactions is provided by ethanol combustion. The system presents two burners: one attached to the reactor (COMB1) and an extra burner (COMB2) that will eventually act under any operating condition of the process.

The proposed structure allows recovering energy from the combustion gases and post reformed gases leaving the reactor. While the main structure of the network is fixed, the design target is to determine the area and operating conditions ensuring feasible operation and an adequate efficiency for different operating scenarios. Three operation scenarios or periods are assessed: nominal design, one-half rated load, and 25% of nominal flow. Specifications for each operational scenario are listed in Table 1. In the nominal case, hydrogen molar flow production is set at 223 mol/h (approximately 5 Nm^3/h). All streams entering the system (water, ethanol, and air) are set at 298 K. The pressure in the reforming line is assumed to be 303.98 kPa; on the other hand, atmospheric conditions were specified in the streams that belong to the combustion section. Pressure losses were considered negligible.

Optimization of problem formulation

A nonlinear optimization problem (NLP) for the processor design was formulated.

$$\min \quad fo = \sum_{ST} w_k f_k(x_k)$$

Table 1 – Process streams specifications.

Scenario	Stream	Molar Flow rate (mol/h)	Temperature (K)
Nominal case	#17	223	
(Period 1)	#12		973
Period 2	#17	111.5	
	#12		973
Period 3	#17	55.75	
	#12		973

Please cite this article in press as: Francesconi JA, et al., Flexible heat exchanger network design of an ethanol processor for hydrogen production. A model-based multi-objective optimization approach, International Journal of Hydrogen Energy (2016), http://dx.doi.org/10.1016/j.ijhydene.2016.10.156

s.t. $h(x_k) = 0$

$g(x_k) \leq 0$ NLP

$x \in \mathbb{R}^n$, $k \in ST$

Here, x represents a vector of continuous variables corresponding to flows, compositions, temperatures, and equipment design parameters. Equality equations represent the process, mainly characterized by the evaluation of properties of the streams and mass and energy balances in equipments. Inequality equations correspond to constraints and specifications of process variables, where fo represents the objective function, generally expressed as a weighted summation of objectives over the k periods. The whole system of equations is evaluated simultaneously over k operative periods or scenarios, grouped into the ST set. Therefore, mass and energy balances should be satisfied for every operational scenario under consideration. Constraints for equipment sizing and system structure link the different scenarios.

The methodology, based on a steady-state model, assumes a monotonic behavior of the system. It is supposed that transitions, from one scenario to another, would occur in a monotonic and smooth way. This hypothesis allows designing of the system without addressing the construction, implementation and resolution of a dynamic model, which would incorporate mathematical complexity to the problem. The monotonic requirement allows guaranteeing that the discrete scenarios provide a convex hull for the search domain, assuring the feasibility of the design during a dynamic transition. This hypothesis is used in the literature [25].

In fuel cell systems, there is a trade-off between efficiency and equipment size (area) [28]. In this paper, we consider two contradictory objectives, efficiency and total heat exchanger area. The objective functions considered in the present work are discussed in "Objective functions" Section.

The problem will be addressed as a multi-objective optimization using the epsilon-constraint approach to sequentially solve multiple single objective optimization problems [29]. In first place, the efficiency level is selected to be optimized getting a maximum bound for the equipment area. Following, the area is converted into an objective and efficiency becomes a constraint. In each subsequent optimization problem, the efficiency constraint level is decreased. In this way, it is possible to guarantee a starting feasible point for each consecutive NLP problem. Finally, a Pareto Optimal solution is achieved.

Therefore, a non-linear multi-period multi-objective mathematical programming model is formulated and solved. A detailed description of model equations and objective functions is shown in the following section.

Mathematical model

Following, the main equations of the model are described. Standard equations for process stream representation are summarized in Appendix A.

Definitions of sets

In order to build a mathematical representation of the system, process streams are divided into three sets: Gaseous Streams (*G*), Liquid Streams (*L*), and Vapor-Liquid Streams (*VL*). The latter represents the case in which the state of the stream is not defined a priori and its condition can change while searching for a solution in the mathematical optimization procedure. In addition, sets for gaseous and liquid compounds are defined as *GC* and *LC* respectively. Sets are summarized in Table 2.

Stream enthalpies

In the process of finding the optimal solution, water streams attached in H1, H2, and H3 exchangers may be in gaseous (vapor), liquid, or both liquid and vapor states. In a mathematical programming framework, it is not possible to define a piecewise continuous function by using an "if-else" structure as in a procedural programming language. Implementation of piecewise continuous functions requires the use of binary variables [26,27], increasing the mathematical complexity of the model. In this work, alternatively, it is proposed a sigmoidal approximation for evaluating enthalpy for streams where their condition was not defined a priori. The sigmoidal approximation is given by the following equation:

$$Hvl_{s,k} = \frac{Hvm_{s,k}(T_{s,k}) + Hlm_{s,k}(T_{s,k})}{2} + \frac{Hvm_{s,k}(T_{s,k}) - Hlm_{s,k}(T_{s,k})}{2}\tanh\left(\frac{T_{s,k} - Tsat(P)}{\theta}\right) \quad (1)$$

This expression, defined for $s \varepsilon VL$, $k \varepsilon ST$, evaluates enthalpy accurately, introducing a very small error if temperature approaches saturation temperature values. Parameter θ controls accuracy; and when taking a value of $\theta = 10^{-6}$, the error is about $2 \cdot 10^{-6}$, as it is shown in Fig. 2.

This expression allows calculating stream vapor fraction as follows:

$$fv_{s,k} = \frac{Hvl_{s,k} - Hlm_{s,k}(T_{s,k})}{Hvm_{s,k}(T_{s,k}) - Hlm_{s,k}(T_{s,k})} \quad (2)$$

Heat exchangers

Overall energy balances for every heat exchanger (HX) are the following:

$$H^{ss}_{out,k} - H^{ss}_{in,k} = Qh_{HX,k} \quad \text{Hot Side (Shell)} \quad (3)$$

$$H^{ts}_{out,k} - H^{ts}_{in,k} = Qc_{HX,k} \quad \text{Cold Side (Tubes)} \quad (4)$$

$$Qh_{HX,k} + Qc_{HX,k} = 0 \quad (5)$$

Thermal load for cold ($Qc_{HX,k}$) and heat ($Qh_{HX,k}$) sides are determined by input (*in*) and output (*out*) enthalpies (*H*) for cold and hot streams in each stage k. It is considered that cold thermal load enters into the tube side (*ts*); and hot gases circulate by shell side (*ss*). Thermal loads are balanced by equation (5).

The logarithmic mean of the temperature difference (*LMTD*) is calculated by using Chen approximation [30].

Please cite this article in press as: Francesconi JA, et al., Flexible heat exchanger network design of an ethanol processor for hydrogen production. A model-based multi-objective optimization approach, International Journal of Hydrogen Energy (2016), http://dx.doi.org/10.1016/j.ijhydene.2016.10.156

Table 2 – Definitions of sets.

Name	Description	Components
G	Gaseous streams	$\{\#11, \#12, \#14, \#15, \#16, \#17, \#18, \#19, \#20, \#21, \#22, \#24, \#25\}$
L	Liquid streams	$\{\#1, \#2, \#3, \#4, \#5, \#13, \#23\}$
VL	Undefined streams (vapor–liquid)	$\{\#6, \#7, \#8, \#9, \#10\}$
GC	Gaseous components	$\{H_2, CO, CO_2, CH_4, CH_3CH_2OH, N_2, O_2, H_2O\}$
LC	Liquid components	$\{H_2O, CH_3CH_2OH\}$
ST	Operational Periods	$\{Period\ 1, Period\ 2, Period\ 3\}$

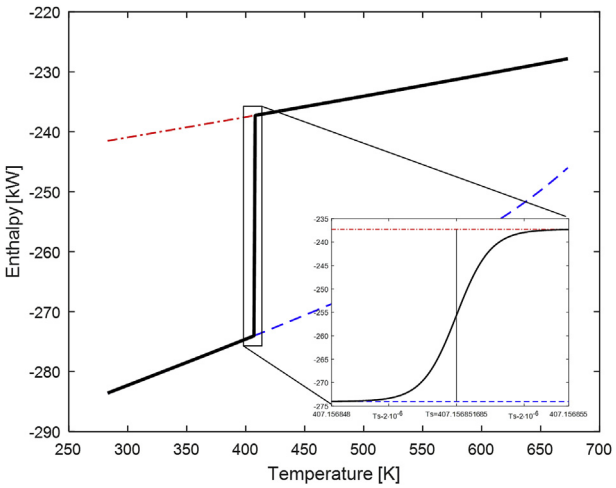

Fig. 2 – Enthalpies for liquid and gas water streams. Sigmoidal approximation and error visualization.

$$LMTD_{HX,k}^{0.3725} = \frac{\left(T_{in,k}^{ss} - T_{out,k}^{ts}\right)^{0.3275} + \left(T_{out,k}^{ss} - T_{in,k}^{ts}\right)^{0.3275}}{2} \quad (6)$$

Constraints for each heat exchanger in relation to the minimum-approach-temperature ($\Delta T_a = 10\ K$) inequality are defined as

$$T_{in,k}^{ss} - T_{out,k}^{ts} \geq \Delta T_a \quad (7)$$

$$T_{out,k}^{ss} - T_{in,k}^{ts} \geq \Delta T_a \quad (8)$$

Heat exchanger area requirement is defined by

$$Area_{HX} = \frac{Qh_{HX,k}}{U_{HX,k}\ LMTD_{HX,k}} \quad (9)$$

It is clear that the area for each heat exchanger is the same for all scenarios under consideration. Global heat transfer coefficient ($U_{HX,k}$) is determined by using typical values for gas (ht_{gas}^0), liquid (ht_{liq}^0), and boiling heat transfer (ht_{boil}^0), considering that these values are representative of the nominal case. Shell side heat transfer (ht_k^{ss}) and tube side heat transfer (ht_k^{ts}) are updated in each period by a flow variation effect. By manipulating Sieder-Tate [31] correlation, it is possible to obtain equations (11) and (12), which update the heat transfer coefficient according to the circulating flow. In the same way, the heat transfer coefficient for shell side is modified by Donahue [32] equation (13). Nevertheless, heat transfer is controlled by the gas circulating into the shell side due to the lower heat transfer value for gases.

$$U_{HX,k} = \left(\frac{1}{h_k^{ts}} + \frac{1}{h_k^{ss}}\right)^{-1} \quad (10)$$

$$h_{gas,k} = \left(\frac{F_k^{ts}}{F_1^{ts}}\right)^{0.8} h_{gas}^0 \quad \text{Tube Side – Gas} \quad (11)$$

$$h_{liq,k} = \left(\frac{F_k^{ts}}{F_1^{ts}}\right)^{0.8} h_{liq}^0 \quad \text{Tube Side – Liquid} \quad (12)$$

$$h_k^{ss} = \left(\frac{F_k^{ss}}{F_1^{ss}}\right)^{0.6} h_{gas}^0 \quad \text{Shell Side} \quad (13)$$

Equation (9) is only applicable to HX4 where global heat transfer coefficient is considered constant along the heat transfer area. To properly evaluate the heat exchanger area when a phase change takes place, it is necessary to reformulate the thermal balance. The total heat load is divided into three zones: liquid ($Q_{HX,k}^L$), gas ($Q_{HX,k}^V$), and boiling ($Q_{HX,k}^B$). Two intermediate temperatures ($T_{1,k}^{ts}$ *and* $T_{2,k}^{ts}$) are introduced and their values are determined to meet intermediate energy balances (Fig. 3). These temperatures fluctuate between input and output values, thus allowing for the balance of internal thermal loads when there is no phase change or a phase change occurs only partially.

$$Qc_{HX,k} = Q_{HX,k}^L + Q_{HX,k}^B + Q_{HX,k}^V \quad (14)$$

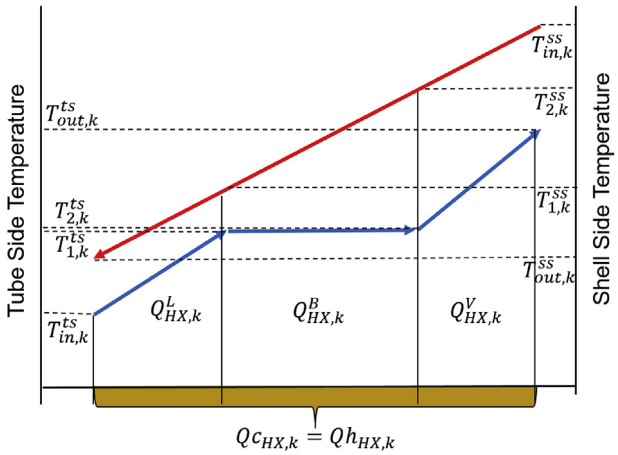

Fig. 3 – Temperatures for a heat exchanger with phase change.

Please cite this article in press as: Francesconi JA, et al., Flexible heat exchanger network design of an ethanol processor for hydrogen production. A model-based multi-objective optimization approach, International Journal of Hydrogen Energy (2016), http://dx.doi.org/10.1016/j.ijhydene.2016.10.156

$$Q^{L}_{HX,k} = (1 - fv_{in,k})\left(H\left(T^{ts}_{!,k}\right) - H\left(T^{ts}_{in,k}\right)\right) \quad (15)$$

$$Q^{B}_{HX,k} = (fv_{out,k} - fv_{in,k})\left(H^{V}(T_{Sat}) - H^{L}(T_{Sat})\right) \quad (16)$$

$$Q^{V}_{HX,k} = fv_{out,k}\left(H\left(T^{ts}_{out,k}\right) - H\left(T^{ts}_{2,k}\right)\right) \quad (17)$$

$$Q^{L}_{HX,k} = H\left(T^{ss}_{1,k}\right) - H\left(T^{ss}_{out,k}\right) \quad (18)$$

$$Q^{B}_{HX,k} = H\left(T^{ss}_{2,k}\right) - H\left(T^{ss}_{1,k}\right) \quad (19)$$

$$Q^{V}_{HX,k} = H\left(T^{ss}_{in,k}\right) - H\left(T^{ss}_{1,k}\right) \quad (20)$$

$$A^{L}_{HX} = \frac{Q^{L}_{HX,k}}{U^{L}_{HX,k}\, LMTD\left(T^{ts}_{in,k}, T^{ts}_{1,k}, T^{ss}_{out,k}, T^{ss}_{1,k}\right)} \quad (21)$$

$$A^{B}_{HX} = \frac{Q^{B}_{HX,k}}{U^{B}_{HX,k}\, LMTD\left(Tsat, T^{ss}_{1,k}, T^{ss}_{2,k}\right)} \quad (22)$$

$$A^{V}_{HX} = \frac{Q^{V}_{HX,k}}{U^{V}_{HX,k}\, LMTD\left(T^{ts}_{2,k}, T^{ts}_{out,k}, T^{ss}_{in,k}, T^{ss}_{2,k}\right)} \quad (23)$$

$$Area_{HX} = A^{L}_{HX,k} + A^{B}_{HX,k} + A^{V}_{HX,k} \quad (24)$$

$$T^{ts}_{in,k} \le T^{ts}_{1,k} \quad (25)$$

$$T^{ts}_{1,k} \le T^{ts}_{2,k} \quad (26)$$

$$T^{ts}_{2,k} \le T^{ts}_{out,k} \quad (27)$$

The area used for transferring sensible heat, for gas (A^{V}_{HX}) or liquid (A^{L}_{HX}), or latent heat during boiling (A^{B}_{HX}), varies in each period, but the total area is always the same. The use of input $(fv_{in,k})$ and output $(fv_{out,k})$ streams vapor fraction in the intermediate thermal balance, equations (15)–(17), allows cancelling each intermediate thermal load when the latter do not occur.

Reformer

Alcohols steam reforming for producing hydrogen involves a complex system of multiple reactions; the obtained hydrogen purity is affected by many undesirable side reactions. Consequently, hydrogen yield depends, in a complex way, on process variables such as pressure, temperature, ratio of reactants, etc., and the catalyst being used [1,2].

The following reactions were considered in the ethanol reformer:

Endothermic decomposition reaction of ethanol

$$C_2H_5OH \rightarrow CO + H_2 + CH_4 \quad \Delta H_{298} = 49.05\ \text{kJ/mol} \quad \text{(Rx1)}$$

Methane reforming

$$CH_4 + H_2O \rightarrow 3H_2 + CO \quad \Delta H_{298} = 206.11\ \text{kJ/mol} \quad \text{(Rx2)}$$

Water gas shift (WGS)

$$CO + H_2O \rightarrow CO_2 + H_2 \quad \Delta H_{298} = -41.1\ \text{kJ/mol} \quad \text{(Rx3)}$$

Reactor reformer is modeled by following an equilibrium approach under isothermal behavior. Decomposition of ethanol into methane is considered as an instantaneous reaction; and, in the mass balance, the extension reaction (ε^{Rx1}_{k}) is matched to input ethanol molar flow. The other extension reactions are determined by equilibrium considerations. Equilibrium expressions are evaluated at the reforming temperature $(T_{Ref,k})$. Equations are defined for $i \in GC,\ j \in \{Rx1,\ Rx2, Rx3\}$.

$$f_{i,\#15,k} = f_{i,\#12,k} + \mu^{j}_{i}\varepsilon^{j}_{k} \quad (28)$$

$$Hgm_{\#12,k}(T_{Ref,k}) - Hgm_{\#15,k}(T_{Ref,k}) = Q_{ref,k} \quad (29)$$

$$Keq_{Rx2,k} = \exp\left(-20.55 - \frac{22920.6}{T_{Ref,k}} + 7.19\ln(T_{Ref,k}) - 2.94\cdot10^{-3}\cdot T_{Ref,k}\right) \quad (30)$$

$$Keq_{Rx3,k} = \exp\left(-12.10 + \frac{5318.69}{T_{Ref,k}} + 1.012\ln(T_{Ref,k}) + 1.144\cdot10^{-4}\cdot T_{Ref,k}\right) \quad (31)$$

$$Keq_{Rx2,k} = \frac{p_{CO,\#12,k}\cdot\left(p_{H_2,\#12,k}\right)^{3}}{p_{CH_4,\#12,k}\cdot p_{H_2O,\#12,k}} \quad (32)$$

$$Keq_{Rx3,k} = \frac{p_{co_2,\#12,k}\cdot p_{H_2,\#12,k}}{p_{CO,\#12,k}\cdot p_{H_2O,\#12,k}} \quad (33)$$

Combustors

Combustors are modeled as adiabatic stoichiometric chemical reactors. Mass and energy balances determine output temperature as an adiabatic temperature flame. The ethanol combustion reaction is considered with a 100% conversion. Air excess is a free variable. Following, equations for COMB2 are presented. COMB1 is modeled in a similar way.

$$CH_3CH_2OH + 3\ O_2 \rightarrow 2\ CO_2 + 3\ H_2O \quad \Delta H_{298} = -1278\ \text{kJ/mol} \quad \text{(Rx4)}$$

$$f_{\#25,i,k} = f_{\#23,i,k} + f_{\#24,i,k} + \mu^{Rx4}_{i}\varepsilon^{Rx4,COMB2}_{k} \quad (34)$$

$$Hgm_{\#25,k} - Hlm_{\#23,k} - Hgm_{\#24,k} = 0 \quad (35)$$

$$AirExcess^{COMB2}_{k} = \frac{f_{\#24,O2,k}}{3\ \varepsilon^{Rx4,COMB2}_{k}} \quad (36)$$

Objective functions

Thermal efficiency (η) of the process is calculated by the ratio of the generated and delivered energy. Lower heating values of hydrogen (LHV_{H_2}) and ethanol (LHV_{EtOL}) are considered.

$$\eta_k = f_{H_2,\#17,k}\cdot LHV_{H_2} \Big/ \left(\left(f_{EtOL,\#1,k} + f_{EtOL,\#13,k} + f_{EtOL,\#22,k}\right)\cdot LHV_{EtOL}\right) \quad (37)$$

Please cite this article in press as: Francesconi JA, et al., Flexible heat exchanger network design of an ethanol processor for hydrogen production. A model-based multi-objective optimization approach, International Journal of Hydrogen Energy (2016), http://dx.doi.org/10.1016/j.ijhydene.2016.10.156

In this work, two objectives are under consideration: efficiency and area. The efficiency objective function (fo_{eff}) is a weighted sum over the different considered periods.

$$fo_{eff} = \sum_{k=1}^{3} w_k \, \eta_k \tag{38}$$

Two alternative cases are analyzed: average efficiency, where each period contributes equally to the objective function (ordinary arithmetic mean), and a weighted efficiency with weigh (w_k) of 0.8 for Period 1 and 0.1 for periods 2 and 3. This latter situation represents an operative case where the system is managed nominally during 80% of time.

The second objective function (fo_{Area}) considers the total area of heat transfer equipment.

$$fo_{Area} = \sum_{i=H1}^{H4} Area_i \tag{39}$$

Resolution methodology

The implementation and resolution of the NLP model was accomplished by means of a mathematical modeling environment and optimization software: General Algebraic Modeling System (GAMS) [33], with CONOPT solver. CONOPT is a feasible path solver based on the generalized reduced gradient method. It represents an efficient and reliable choice for highly nonlinear problems.

Considering an epsilon-constraint approach, the first step is to determine the minimal area requirement that allows obtaining the maximum efficiency. This step is performed by sequentially solving two NLP problems. First, NLP-1 finds the maximum efficiency.

$$\text{NLP}-1 \quad \text{s.t.} \quad \begin{array}{l} max\, fo_{eff} \\ h(x_k) = 0 \\ g(x_k) \le 0 \end{array} \quad x \in \mathbb{R}^n,\ k \in ST$$

Following, a second NLP is solved to determine the minimum area for the previous efficiency (fo_{eff}^{Max}) determined in NLP-1.

$$\text{NLP}-2 \quad \text{s.t.} \quad \begin{array}{l} min\, fo_{Area} \\ h(x_k) = 0 \\ g(x_k) \le 0 \\ fo_{eff} = fo_{eff}^{Max} \end{array} \quad x \in \mathbb{R}^n,\ k \in ST$$

Subsequently, Problem NLP-3 is repeatedly solved by decreasing gradually the epsilon value (ε) in the constraint for the efficiency inequality.

$$\text{NLP}-3 \quad \text{s.t.} \quad \begin{array}{l} min\, fo_{Area} \\ h(x_k) = 0 \\ g(x_k) \le 0 \\ fo_{eff} > \varepsilon \end{array} \quad x \in \mathbb{R}^n,\ k \in ST$$

It is worth noting that the system is represented by a large-scale nonconvex nonlinear mathematical model, CONOPT solver based on a local deterministic optimization algorithm may not converge to the global minimum/maximum of the problem. Under this condition, the results plotted in Fig. 4 certainly represent a locally Pareto Optimal. This limitation could be overcome using a global optimization algorithm, but with a very high computational cost and prohibited computation time in the case under study. To approach locally optimal points to global ones, the following strategy was applied. The epsilon-constraint methodology starts from the best solution founded from solving several times the NLP-1 and NLP-2 problems. This optimal search was carried out by means of different seed values or initial points. Once that the most favorable solution was detected, in the subsequent NLP solvers the value of epsilon is slightly decreased. In conclusion, the Pareto curve was obtained after solving about of 2500 NLP sub-problems, decreasing in each new NLP problem the constraint value for the efficiency by 1e-4. This methodology does not guarantee global optimality, but gives useful and worthy results close to global ones.

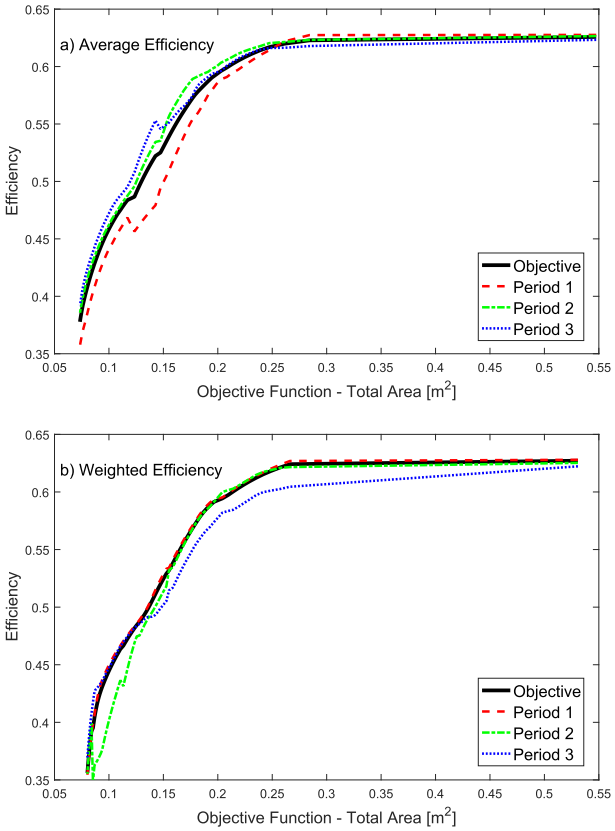

Fig. 4 – Multi-objective optimization. Efficiency *vs.* area. a) Average efficiency. b) Weighted efficiency.

Results

Table 3 shows design values for heat exchangers, i.e., the heat exchanger heat transfer area obtained in the solution of the second NLP problem (NLP-2) for both analyzed efficiency functions. These solutions represent the case with the largest area and maximum efficiency. Comparatively, both area requirements are similar for Average and Weighted cases.

Table 4 summarizes the values for the operating variables obtained by solving the optimization problem. It is worth noting that efficiency values remain in the order of 63% in the three considered scenarios and for both efficiency objectives (Average and Weighted).

Please cite this article in press as: Francesconi JA, et al., Flexible heat exchanger network design of an ethanol processor for hydrogen production. A model-based multi-objective optimization approach, International Journal of Hydrogen Energy (2016), http://dx.doi.org/10.1016/j.ijhydene.2016.10.156

Table 3 – Heat exchangers sizing for maximum efficiency cases.

	Area (m^2)				Total (fo_{Area})	fo_{eff}
	HX1	HX2	HX3	HX4		
Average	0.1114	0.1028	0.0538	0.2795	0.5476	0.6271
Weighted	0.0874	0.0933	0.0873	0.2628	0.5308	0.6258

Validation and verification of the results obtained were done using a commercial process simulation software. Simulations of the three scenarios were performed specifying input temperatures and flows. The simulated data obtained using Aspen HYSYS showed a very good agreement with the values presented in Tables 5 and 6. This comparison verified the model implementation in GAMS, and the use of the sigmoidal approximation on the calculation of enthalpy.

Structurally, it should be mentioned that the secondary burner does not operate in the case of nominal load (Period 1) for the Average Efficiency case. Water supply is different in each stage; the system uses the three insertion points for the first scenario and in Periods 1 to 3 for the Weighted case. These results show that the proposed structure provides the process with flexibility so as to achieve a maximum value of efficiency in all operating conditions.

In Tables 5 and 6, temperature values corresponding to hot and cold loads of each exchanger are detailed, italicized values represent specifications.

Heat exchanger HX4 represents the equipment with the largest area in both cases. Phase change takes place mainly into the second heat exchanger, as shown in Table 7, where fraction vapor for the set of liquid–vapor streams is summarized.

Below, there is a discussion on the results obtained from the solution of the multi-objective problem by sequentially running the NLP-3 problem with both efficiencies (Average and Weighted) under consideration.

Fig. 4 shows the Pareto Optimal chart comparing energetic efficiency *vs.* area. System performances for each operative period and efficiency objective function are plotted. When analyzing the Average Efficiency case (Fig. 4a), efficiencies present similar values around 62% for above 0.25 m^2. For the second case, as it was expected, the objective function curve is

Table 5 – Process temperatures for the average efficiency case [K]. Italicized values represent temperature specifications.

Heat exchanger		Nominal design period 1		Operation at 50% period 2		Operation at 25% period 3	
H1	#3-#6	298.0	610.6	298.0	407.1	298.0	407.1
	#16-#17	767.1	473.0	890.6	473.0	874.7	473.0
H2	#7-#8	407.1	600.02	407.1	835.9	407.1	812.4
	#21-#22	1010.5	417.1	1162.9	417.1	1035.2	417.1
H3	#9-#10	407.1	666.1	835.9	961.7	812.4	963.0
	#15-#16	973.0	767.1	973.0	890.6	973.0	874.7
H4	#11-#12	473.0	973.0	699.8	973.0	699.7	973.0
	#19-#20	1487.9	1010.5	1101.9	710.6	1008.6	723.8

Table 6 – Process temperatures for the weighted efficiency case [K]. Italicized values represent temperature specifications.

Heat exchanger		Nominal design period 1		Operation at 50% period 2		Operation at 25% period 3	
H1	#3-#6	298.0	521.1	298.0	407.1	298.0	464.7
	#16-#17	698.5	473.0	799.9	473.0	668.9	473.0
H2	#7-#8	407.1	522.0	407.1	673.5	407.1	463.5
	#21-#22	1101.0	417.1	1093.8	417.1	952.4	417.4
H3	#9-#10	407.1	776.1	673.5	942.7	407.4	870.7
	#15-#16	973.0	698.5	973.0	799.9	973.0	668.9
H4	#11-#12	557.9	973.0	684.8	973.0	627.9	973.0
	#19-#20	1281.5	681.2	1067.3	712.8	994.3	668.3

Table 7 – Vapor fraction for liquid–vapor streams.

Period	Stream						
	H1		H2		H3		
	#3	#6	#7	#8	#9	#10	
Period 1	0	1.0	0.28	1.0	0.92	1.0	Average efficiency
Period 2	0	0.38	0.38	1.0	1.0	1.0	
Period 3	0	0.52	0.35	1.0	1.0	1.0	
Period 1	0	1.0	0.15	1.0	0.93	1.0	Weighted efficiency
Period 2	0	0.33	0.25	1.0	1.0	1.0	
Period 3	0	1.0	0.08	1.0	0.97	1.0	

Table 4 – Results obtained. Operative variables.

Stream	Variable	Average efficiency			Weighted efficiency		
		Design nominal	Operation at 50%	Operation at 25%	Design nominal	Operation at 50%	Operation at 25%
#1	*Ethanol to reformer (mol/h)*	44.64	22.40	11.22	44.73	22.41	11.22
	water/ethanol ratio	7.68	7.56	7.51	7.61	7.54	7.47
#3	Water flow [mol/h]	100.58	167.29	65.33	80.79	145.09	18.02
#4	Water flow [mol/h]	181.91	1.99	18.94	215.52	23.94	61.04
#5	Water flow [mol/h]	60.44	0.00	0.00	44.45	0.00	4.91
#13	Ethanol to burner 1 [mol/h]	24.94	8.05	4.46	17.62	8.51	4.64
#14	Air excess burner 1 [%]	28	52	96	28	70	107
#23	Ethanol to burner 2 [mol/h]	0	4.38	1.83	7.20	3.99	1.67
#24	Air excess burner 2 [%]	–	15	15	15	15	15
	Efficiency	62.75	62.65	62.33	62.79	62.52	62.22

Please cite this article in press as: Francesconi JA, et al., Flexible heat exchanger network design of an ethanol processor for hydrogen production. A model-based multi-objective optimization approach, International Journal of Hydrogen Energy (2016), http://dx.doi.org/10.1016/j.ijhydene.2016.10.156

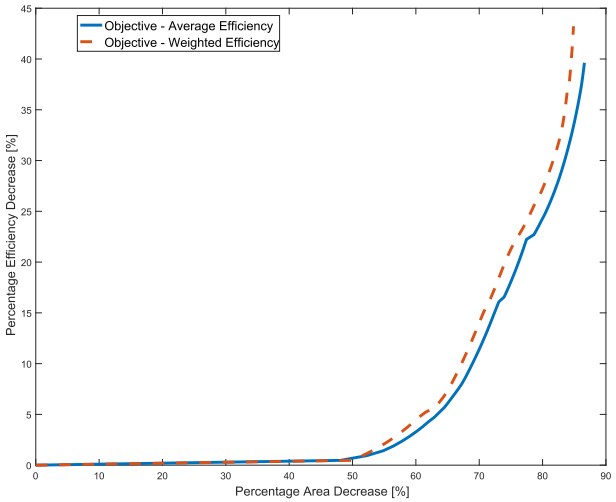

Fig. 5 – Relationship between area and efficiency decrease.

overlapped with Period 1 performance due to their high contribution to the weighted efficiency (Fig. 4b).

When comparing both efficiency functions, the weighted efficiency case required a larger area for the same efficiency value.

From these curves, in a 0.25–0.36 m^2 area range, it can be clearly noted that efficiency approaches are asymptotical to the maximum value (63%). This implies that a 50% reduction of the required area only diminishes efficiency by 1%. The

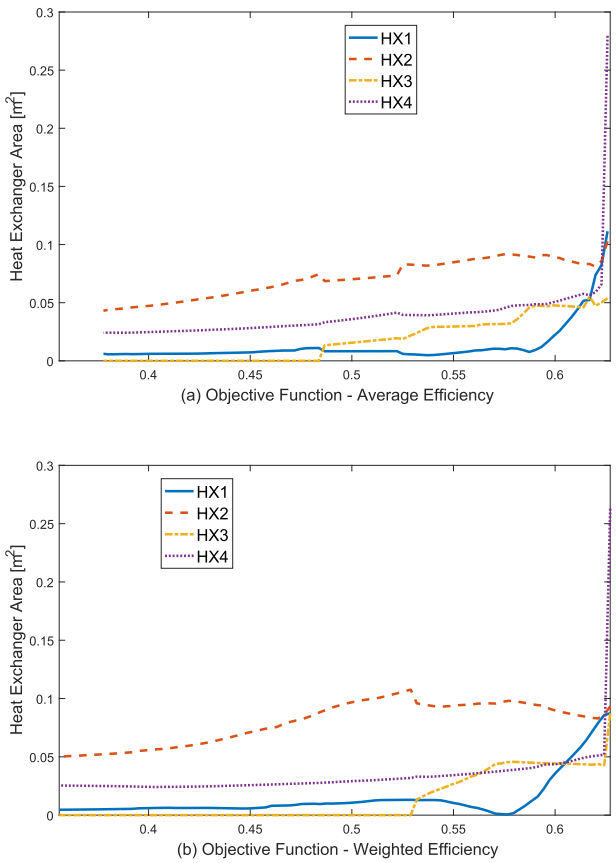

Fig. 6 – Area variation for each heat exchanger during the pareto optimal construction.

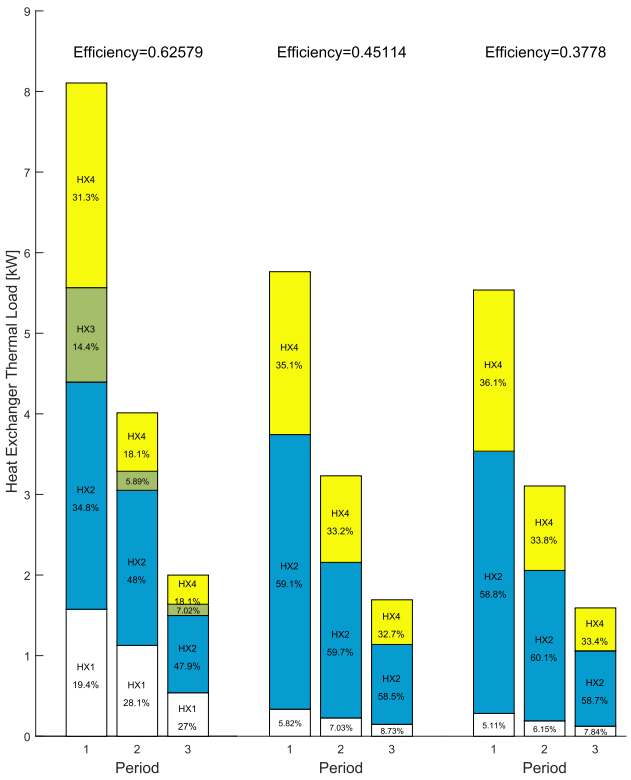

Fig. 7 – Thermal load distribution for different values of efficiency.

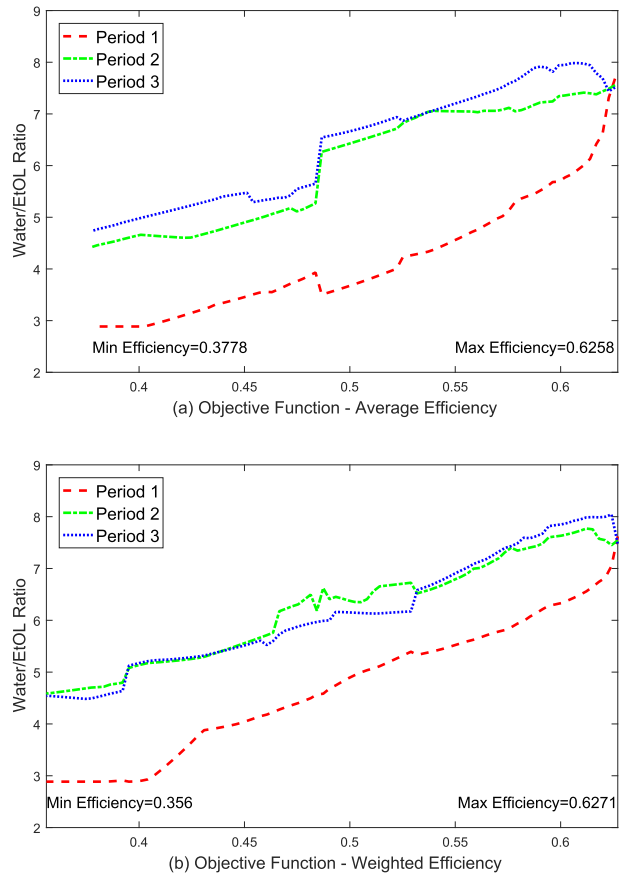

Fig. 8 – Variation of the reactant ratio as a function of system efficiency.

Please cite this article in press as: Francesconi JA, et al., Flexible heat exchanger network design of an ethanol processor for hydrogen production. A model-based multi-objective optimization approach, International Journal of Hydrogen Energy (2016), http://dx.doi.org/10.1016/j.ijhydene.2016.10.156

relationship between area and efficiency reductions is more clearly depicted in Fig. 5, where both operating scenarios are compared (Average and Weighted).

Fig. 6 shows the area of each heat exchanger in relation to efficiency. There exists a limit value for which the HX3 is no longer necessary. This limit is presented below 48% or 53%, according to the objective function being considered. HX2 is the largest area equipment, except at maximum efficiency where HX4 presents a significant superior value.

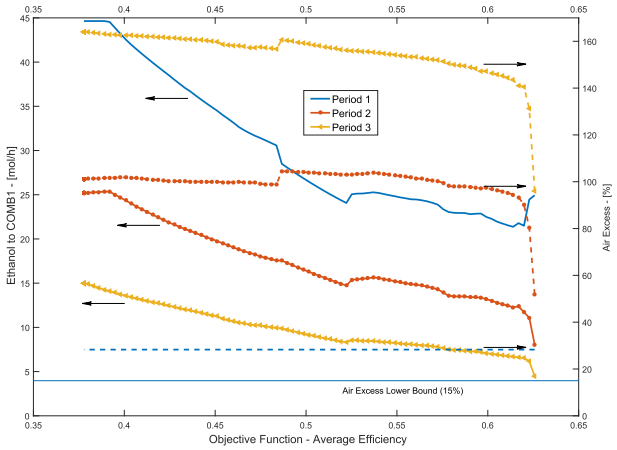

Fig. 9 – Ethanol flow rate and air excess percentage for the average efficiency case.

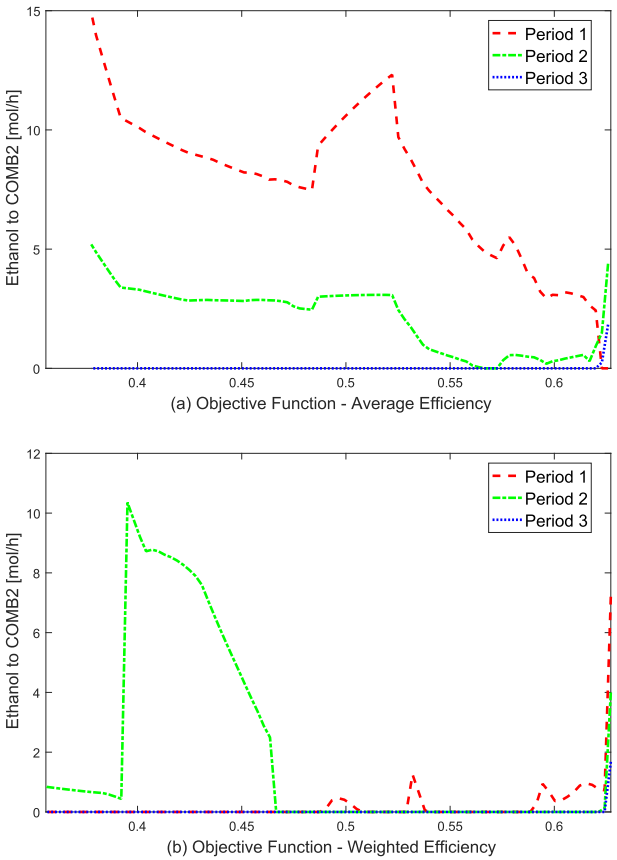

Fig. 10 – Variation of ethanol flow rate for COMB2 as a function of system efficiency.

Fig. 7 shows the heat exchanger thermal load in each period for three selected efficiency values. HX2 manages the greatest load in all cases since it is where the phase change mainly takes place.

It is also interesting to note the variation on operating variables when the total area is reduced. The ratio of reactant molar flow rates for both efficiency objective functions is compared in Fig. 8. It is shown that the reactant ratio takes values between 3 and 8; and the low load operation (Period 3) generally requires higher values to keep system efficiency.

The fuel flow to be burnt is analyzed in Figs. 9 and 10. They show an increase in the ethanol flow to the main burner while efficiency decreases. Moreover, while efficiency decreases in Periods 2 and 3, the air excess rises (Fig. 9).

Ethanol flow into the second burner clearly reveals that this operation might not be necessary, at least when the weighted efficiency objective function is considered (Fig. 10b). Fig. 10a, corresponding to the average function, shows that the second burner is not active in Period 3. The behavior of this operational variable is markedly different in both scenarios of the analyzed efficiency objective functions.

Conclusions

The application of mathematical programming techniques provided the conceptual design of an ethanol processor, determining operational variable values and keeping maximum efficiency within acceptable values (about 63%) for the three scenarios under consideration. Moreover, the NLP mathematical model allowed validating the operability and flexibility of the proposed heat exchanger network and process structure in the range of specified flows. It is concluded that with multi-objective methodology a 50% reduction from the maximum area only decreases the efficiency value by 1%. From the structural point of view, results also showed that it is possible to remove a heat exchanger without compromising operability but jeopardizing system performance.

Although it is not feasible to guarantee global optimality due to the high nonlinearity of the mathematical model, the rigorous physical-chemical approach ensures technical operability. Although the quantitative results are only valid to those scenarios considered throughout this work, the methodology can be extended to other systems and case studies.

Acknowledgments

The authors are grateful for the financial support provided by Consejo Nacional de Investigaciones Científicas y Técnicas (CONICET), Agencia Nacional de Promoción Científica y Tecnológica (ANPCyT, grant numbers PICT-2012-1863 and PICT-2013-1980) of Argentina, and Universidad Nacional del Litoral (UNL).

Nomenclature

G	Gaseous streams set
L	Liquid streams set
VL	Vapor–liquid streams set

Please cite this article in press as: Francesconi JA, et al., Flexible heat exchanger network design of an ethanol processor for hydrogen production. A model-based multi-objective optimization approach, International Journal of Hydrogen Energy (2016), http://dx.doi.org/10.1016/j.ijhydene.2016.10.156

GC	Gaseous compounds set
LC	Liquid compounds set
ST	Operational periods set
T	Temperature, K
P	Total pressure, kPa
p	Partial pressure, kPa
x	Liquid phase molar fraction
y	Gas phase molar fraction
f	Component molar flow rate, mol/h
F	Total molar flow rate, mol/h
H	Enthalpy, kW
Hgm	Gaseous stream enthalpy, W
hg	Gaseous component enthalpy, W
Hlm	Liquid stream enthalpy, W
hl	Liquid component enthalpy, W
Cpl	Liquid component heat capacity, Joule/(mol·K)
Cpg	Gas component heat capacity, Joule/(mol·K)
$\Delta Hvap$	Enthalpy of vaporization, Joule/mol
ΔH^0_{form}	Enthalpy of formation, Joule/mol
Tsat	Saturation temperature, K
fv	Vapor fraction
Qh	Heat thermal load, W
Qc	Cold thermal load, W
LMTD	Logarithmic mean temperature difference, K
U	Global heat transfer coefficient, W/(m^2·K)
ht^0_{gas}	Gas heat transfer coefficient, W/(m^2·K)
ht^0_{liq}	Liquid heat transfer coefficient, W/(m^2·K)
ht^0_{boil}	Boiling heat transfer coefficient, W/(m^2·K)
A	Heat exchanger area, m^2

Greek letters

α	Antoine equation coefficient
δ	Vaporization enthalpy equation coefficient
θ	Sigmoidal equation error control

Subscripts

k	Period or stage of operation
i	Compound
s	Stream
HX	Heat exchanger
in	input
out	output
1	Heat exchanger internal section
2	Heat exchanger internal section

Superscripts

ts	Tube side
ss	Shell side
L	Liquid heat exchanger zone
V	Vapor heat exchanger zone
B	Boiling heat exchanger zone

Appendix A. Standard equations for stream definition.

Temperature ($T_{s,k}$), pressure (P), and compositions for liquid phase ($x_{i,s,k}$) or gas phase ($y_{i,s,k}$) define every stream of the system. In addition, partial pressure ($p_{i,s,k}$), component molar flows ($f_{i,s,k}$) and total molar flow ($F_{s,k}$) are related by the following equations for all sets of streams. Total pressure is considered to remain constant for the whole system.

$$p_{i,s,k} = y_{i,s,k} \cdot P \tag{A1}$$

$$f_{i,s,k} = y_{i,s,k} F_{s,k} \tag{A2}$$

$$F_{s,k} = \sum_{i=1}^{\#S} f_{i,s,k} \tag{A3}$$

where $s \in G \wedge L \wedge LV, i \in GC \wedge LC$ and $k \in ST$, $\#S$ represent the cardinality of the corresponding set. Enthalpy values are calculated according to stream temperature and composition. Mathematical expressions vary depending on the state of stream: gas or liquid. For gaseous streams, enthalpy of stream s at period k ($Hgm_{s,k}$) is determined by the enthalpy of compound i in gaseous phase ($hg_{i,s,k}$) and the component molar flow rate ($f_{i,s,k}$). The following equations are defined for $\in G, i \in CG,\ k \in ST$:

$$Hgm_{s,k} = \sum_{i}^{\#CG} \left(f_{i,s,k} \cdot hg_{i,s,k} \right) \Big/ 3600 \tag{A4}$$

$$hg_{i,s,k} = \Delta H^0_{form,i} + \int_{T_0}^{T_{s,k}} Cpg_i(T)dT \tag{A5}$$

Enthalpy in liquid phase ($Hlm_{s,k}$) is evaluated, taking the gas at the temperature of $T_0 = 298$ K as a reference. Saturation temperature of pure compounds is determined by Antoine equation. Then, the pure liquid enthalpy ($hl_{i,s,k}$) is calculated as follows:

$$\log(P) = \frac{\alpha_{A,i} + \alpha_{B,i}}{\alpha_{C,i} + Tsat_i} + \alpha_{D,i} \log(Tsat_i) + \alpha_{E,i} (Tsat_i)^{\alpha_{F,i}} \tag{A6}$$

$$\log(\Delta Hvap_i) = \log(\delta_{A,i}) + \log\left(1 - \frac{Tsat_i}{Tc_i}\right)\delta_{B,i} + \delta_{C,i}\frac{Tsat_i}{Tc_i} + \delta_{D,i}\left(\frac{Tsat_i}{Tc_i}\right)^2 + \delta_{E,i}\left(\frac{Tsat_i}{Tc_i}\right)^3 \tag{A7}$$

$$hl_{i,s,k} = \Delta H^0_{form,i} + \int_{T_0}^{Tsat_i} Cpg_i(T)dT - \Delta Hvap_i - \int_{T_{s,k}}^{Tsat_i} Cpl_i(T)dT \tag{A8}$$

$$Hlm_{s,k} = \frac{f_{i,s,k} \cdot hl_{i,s,k}}{3600} \tag{A9}$$

where P represents pressure, $Tsat$ is saturation temperature, $\Delta Hvap_i$ is latent energy at $Tsat$, Cpg_i is heat capacity for compound i in gas phase, and Cpl_i is liquid heat capacity for compound i. These equations are defined for $s \in L, i \in CL,\ k \in ST$. Liquid streams are composed of only one component, i.e. either water or ethanol. As a consequence, it is not necessary to apply equilibrium liquid vapor on the model.

REFERENCES

[1] García EY, Laborde MA. Hydrogen production by the steam reforming of ethanol: thermodynamic analysis. Int J

Please cite this article in press as: Francesconi JA, et al., Flexible heat exchanger network design of an ethanol processor for hydrogen production. A model-based multi-objective optimization approach, International Journal of Hydrogen Energy (2016), http://dx.doi.org/10.1016/j.ijhydene.2016.10.156

Hydrogen Energy 1991;16:307–12. http://dx.doi.org/10.1016/0360-3199(91)90166-G.
[2] Mariño F, Boveri M, Baronetti G, Laborde M. Hydrogen production from steam reforming of bioethanol using Cu/Ni/K/ã-Al_2O_3 catalysts. Effect of Ni. Int J Hydrogen Energy 2001;26:665–8. http://dx.doi.org/10.1016/S0360-3199(01)00002-7.
[3] Xuan J, Leung MKH, Leung DYC, Ni M. A review of biomass-derived fuel processors for fuel cell systems. Renew Sust Energ Rev 2009;13:1301–13. http://dx.doi.org/10.1016/j.rser.2008.09.027.
[4] Lopes DG, da Silva EP, Pinto CS, Neves Jr NP, Camargo JC, Ferreira PFP, et al. Technical and economic analysis of a power supply system based on ethanol reforming and PEMFC. Renew Energy 2012;45:205–12. http://dx.doi.org/10.1016/j.renene.2012.03.006.
[5] Datta R, Maher MA, Jones C, Brinker RW. Ethanol - the primary renewable liquid fuel. J Chem Technol Biot 2011;86:473–80. http://dx.doi.org/10.1002/jctb.2580.
[6] Sarris D, Papanikolaou S. Biotechnological production of ethanol: biochemistry, processes and technologies. Eng Life Sci 2016;16:307–29. http://dx.doi.org/10.1002/elsc.201400199.
[7] Aditiya HB, Mahlia TMI, Chong WT, Nur H, Sebayang AH. Second generation bioethanol production: a critical review. Renew Sust Energ Rev 2016;66:631–53. http://dx.doi.org/10.1016/j.rser.2016.07.015.
[8] Li M-F, Yang S, Sun R-C. Recent advances in alcohol and organic acid fractionation of lignocellulosic biomass. Bioresour Technol 2016;200:971–80. http://dx.doi.org/10.1016/j.biortech.2015.10.004.
[9] Francesconi JA, Mussati MC, Mato RO, Aguirre PA. Analysis of the energy efficiency of an integrated ethanol processor for PEM fuel cell systems. J Power Sources 2007;167:151–61. http://dx.doi.org/10.1016/j.jpowsour.2006.12.109.
[10] Godat J, Marechal F. Optimization of a fuel cell system using process integration techniques. J Power Sources 2003;118:411–23. http://dx.doi.org/10.1016/S0378-7753(03)00107-1.
[11] Perna A. Hydrogen from ethanol: theoretical optimization of a PEMFC system integrated with a steam reforming processor. Int J Hydrogen Energy 2007;32:1811–9. http://dx.doi.org/10.1016/j.ijhydene.2006.08.058.
[12] Manzolini G, Tosti S. Hydrogen production from ethanol steam reforming: energy efficiency analysis of traditional and membrane processes. Int J Hydrogen Energy 2008;33:5571–82. http://dx.doi.org/10.1016/j.ijhydene.2008.06.029.
[13] Salemme L, Menna L, Simeone M. Thermodynamic analysis of ethanol processors – PEM fuel cell systems. Int J Hydrogen Energy 2010;35:3480–9. http://dx.doi.org/10.1016/j.ijhydene.2010.01.119.
[14] Oliva DG, Francesconi JA, Mussati MC, Aguirre PA. Modeling, synthesis and optimization of heat exchanger networks. Application to fuel processing systems for PEM fuel cells. Int J Hydrogen Energy 2011;36:9098–114. http://dx.doi.org/10.1016/j.ijhydene.2011.04.097.
[15] Francesconi JA, Mussati MC, Aguirre PA. Analysis of design variables for water-gas-shift reactors by model-based optimization. J Power Sources 2007;173:467–77. http://dx.doi.org/10.1016/j.jpowsour.2007.04.048.
[16] Kamarudin SK, Daud WRW, Md. Som A, Takriff MS, Mohammad AW. Synthesis and optimization of a PEM fuel cell system via reactor-separation network (RSN). J Power Sources 2006;159:1194–204. http://dx.doi.org/10.1016/j.jpowsour.2005.11.087.
[17] Ang SMC, Fraga ES, Brandon NP, Samsatli NJ, Brett DJL. Fuel cell systems optimisation – methods and strategies. Int J Hydrogen Energy 2011;36:14678–703. http://dx.doi.org/10.1016/j.ijhydene.2011.08.053.
[18] Grossmann IE, Halemane KP, Swaney RE. Optimization strategies for flexible chemical processes. Comp Chem Eng 1983;7:439–62. http://dx.doi.org/10.1016/0098-1354(83)80022-2.
[19] Yunt M, Chachuat B, Mitsos A, Barton PI. Designing man-portable power generation systems for varying power demand. AIChE J 2008;54:1254–69. http://dx.doi.org/10.1002/aic.11442.
[20] Linnhoff BA. User guide on process integration for the efficient use of energy. Institution of Chemical Engineers; 1994.
[21] Furman KC, Sahinidis NV. A critical review and annotated bibliography for heat exchanger network synthesis in the 20th century. Ind Eng Chem Res 2002;41:2335–70. http://dx.doi.org/10.1021/ie010389e.
[22] Floudas CA, Grossmann IE. Synthesis of flexible heat exchanger networks for multiperiod operation. Comp Chem Eng 1986;10:153–68.
[23] Verheyen W, Zhang N. Design of flexible heat exchanger network for multi-period operation. Chem Eng Sci 2006;61:7730–53. http://dx.doi.org/10.1016/j.ces.2006.08.043.
[24] Yee TF, Grossmann IE. Simultaneous optimization models for heat integration—II. Heat exchanger network synthesis. Comp Chem Eng 1990;14:1165–84. http://dx.doi.org/10.1016/0098-1354(90)85010-8.
[25] Aaltola J. Simultaneous synthesis of flexible heat exchanger network. Appl Therm Eng 2002;22:907–18. http://dx.doi.org/10.1016/S1359-4311(02)00008-X.
[26] Ponce-Ortega JM, Jiménez-Gutiérrez A, Grossmann IE. Optimal synthesis of heat exchanger networks involving isothermal process streams. Comp Chem Eng 2008;32:1918–42. http://dx.doi.org/10.1016/j.compchemeng.2007.10.007.
[27] Kamath RS, Biegler LT, Grossmann IE. Modeling multistream heat exchangers with and without phase changes for simultaneous optimization and heat integration. AIChE J 2012;58:190–204. http://dx.doi.org/10.1002/aic.12565.
[28] Mitsos A, Chachuat B, Barton PI. What is the design objective for portable power generation: efficiency or energy density? J Power Sources 2007;164:678–87. http://dx.doi.org/10.1016/j.jpowsour.2006.10.088.
[29] Rangaiah GP. Multi-objective optimization: techniques and applications in chemical engineering. World Scientific; 2009.
[30] Chen JJJ. Comments on improvements on a replacement for the logarithmic mean. Chem Eng Sci 1987;42:2488–9. http://dx.doi.org/10.1016/0009-2509(87)80128-8.
[31] Sieder EN, Tate GE. Heat transfer and pressure drop of liquids in tubes. Ind Eng Chem 1936;28:1429–35. http://dx.doi.org/10.1021/ie50324a027.
[32] Donohue DA. Heat transfer and pressure drop in heat exchangers. Ind Eng Chem 1949;41:2499–511. http://dx.doi.org/10.1021/ie50479a030.
[33] GAMS Development Corporation. General algebraic modeling system (GAMS) release 24.2.1. Washington, DC, USA. 2013. p. 2013.

Please cite this article in press as: Francesconi JA, et al., Flexible heat exchanger network design of an ethanol processor for hydrogen production. A model-based multi-objective optimization approach, International Journal of Hydrogen Energy (2016), http://dx.doi.org/10.1016/j.ijhydene.2016.10.156